International Journal of Applied Power Engineering (IJAPE)
Vol. 15, No. 2, June 2026, pp. 646~662
ISSN: 2252-8792, DOI: 10.11591/ijape.v15.i2.pp646-662

Analyzing the ability of capacitor energy in a modular multilevel converter to support inertia in an AC system

Dunya Sh. Wais, Huda A. Abbood
Department of Electrical Engineering, College of Engineering, Mustansiriyah University, Baghdad, Iraq

Article Info

Article history:

Received Oct 6, 2025
Revised Jan 14, 2026
Accepted Mar 12, 2026

Keywords:

Capacitor energy
Fractional response
Inertia constant
Modular multilevel converter
Support strength

ABSTRACT

Flexible DC transmission systems based on modular multilevel converters have the potential to support the inertia of AC power grids by using sub-module capacitor energy storage. However, existing studies generally believe that the inertia provided by flexible DC systems is limited by their energy storage time constants, which is weaker than that of synchronous motors, and lacks quantitative indicators to measure their support strength. Introducing the flexible-DC equivalent inertia constant (FDEIC) as a precise metric for assessing inertia support under different management schemes, this research presents a new analytical framework based on frequency responses. Results show that the inertial response is influenced by control bandwidth, DC-voltage dynamics, and circulating-current behaviour. A more generalized multi-terminal FDEIC is created to account for the impact of raised total capacitor energy, and the theory is further expanded to cover DC grids with more than one terminal. A three-terminal flexible DC grid simulation model is built in the PSCAD environment, and the simulation results verify the effectiveness of the proposed quantitative analysis method.

Corresponding Author:

Dunya Sh. Wais
Department of Electrical Engineering, College of Engineering, Mustansiriyah University
Baghdad, Iraq
Email: dunya.sh.wais@uomustansiriyah.edu.iq

1. INTRODUCTION

The modular multilevel converter based high voltage direct current (MMC-HVDC) technology has the advantages of strong scalability, high controllability, direct access and transmission of wind and solar power generation, and the ability to supply power to weak AC grids and even passive systems. It is currently a relatively advanced transmission technology [1]-[7].

With the access of a high proportion of power electronic devices, the traditional power system with synchronous generator (SG) as the main power source is gradually transforming into a low-inertia weak grid, and the system frequency stability is constantly weakening [8], [9]. Under traditional flexible DC control, modular multilevel converter (MMC) cannot respond to the frequency changes of the AC system, nor can it simulate the synchronous motor to provide inertia for the system, so it is difficult to support the grid frequency stability [10], [11]. How to give full play to the support capability of MMC in the flexible DC system to actively support the frequency of the receiving AC system has become one of the key technical problems that urgently need to be solved in the construction of new power systems [12], [13].

There are many studies on the frequency support strategy of MMC for AC power grid. The study in [14] summarize the common grid-following and grid-building control strategies and analyze their support performance and performance for AC power grid. Khan *et al.* [15] proposes a control scheme that can provide inertia and damping for the two-end grids for the back-to-back MMC-HVDC system, and embeds a

new support mode selection algorithm. Mei *et al.* [16] proposes an adaptive virtual inertia frequency regulation strategy, which increases the inertia coefficient of MMC when the DC deviation is small, and decreases it when it is small, so that it has a better inertia support effect on the AC system in the early stage of frequency fluctuation. Wang *et al.* [17] deeply analyzes the difference between the inertia support function and the primary frequency regulation function of the virtual synchronous generator (VSG) in the power grid, and analyzes the effect of VSG control on frequency changes when severe load disturbance occurs in the large power grid.

In the above research, the supporting power of MMC for the AC system on the disturbance side mainly comes from the AC grid connected to other converter stations in the flexible DC system. There are many discrete sub-module capacitors inside the MMC. If the energy inside can be flexibly and effectively utilized, the MMC's own energy storage alone can provide a certain support effect on the grid.

In order to further utilize the MMC capacitor energy, Zhu *et al.* [18], [19] use capacitor energy to simulate the rotor kinetic energy of the synchronous motor to support the grid inertia, but they use the traditional double closed-loop vector control strategy, and the capacitor voltage is coupled with the DC voltage, which limits the utilization of capacitor energy. Liu *et al*. [20] uses adaptive damping and inertia coefficients to improve the support capacity of capacitor energy, but its capacitor voltage is still related to the DC voltage. Yang *et al.* [21] uses a capacitor energy synchronization loop to replace the power synchronization loop in the traditional grid control to improve stability, but the reference believes that the capacitor energy support effect is extremely small, so it is only used for synchronization with the grid. Singh *et al.* [22] proposes an MMC active energy control strategy, which mathematically decouples the DC voltage and capacitor voltage, and improves the energy utilization margin and control flexibility compared to traditional control. Zhang *et al.* [23], [24]. According to Singh *et al.* [22], it looks at adaptive and intelligent control strategies for power-electronic converters that work in low-inertia grids. It shows how adaptive, predictive, and AI-based solutions improve frequency stability, virtual inertia emulation, and strength when the grid is unpredictable. Some of the biggest problems are making control more complicated, limiting real-time implementation, and making sure stability throughout a wide range of operating situations.

However, the above MMC energy utilization strategies have not been able to quantitatively calculate the actual support strength of MMC for the power grid, and it is difficult to quantify the support effect. Although most existing studies believe that the inertia constant of MMC is only about 40 ms [21], which is very small compared to the effect of synchronous motors, it is mainly obtained by analogy with the energy storage time constant of MMC, and does not consider the impact of actual grid characteristics and MMC control strategies on support capacity.

In order to quantitatively analyze the grid inertia after a high proportion of new energy and power electronic equipment is connected, the Sun *et al.* [9] defines the generalized inertia of the grid by using the ratio of the generalized kinetic energy of the AC system to the total capacity, which covers all forms of inertia in the system, but is not suitable for analyzing the inertia support capacity of the flexible DC MMC alone. Yang *et al*. [25] proposes an MMC inertia constant considering the penetration rate of new energy and analyzes the frequency response of the AC grid after the introduction of MMC inertia. However, the motor speed is equivalent to the capacitor voltage during the calculation, which is inconsistent with the physical definition of the inertia constant. In addition, the total capacity of the grid is used as the base value for power calculation, which makes it difficult to reflect the actual effect of capacitor energy on grid inertia. Kim *et al.* [26] derives the inertia constant of the converter station by analogy between capacitor energy and the kinetic energy of the synchronous motor rotor. However, this literature only considers the impact of the third harmonic injection on the number of submodules put into operation, and does not analyze the improvement of the energy utilization range brought by the decoupling of DC voltage and capacitor voltage. It also does not consider the different abilities of capacitors to absorb and release energy, and the obtained inertia constant is too small.

In view of the above problems, this paper first starts from the frequency response model of the flexible DC transmission system, derives the quantitative analysis method of the inertia support capacity of a single flexible DC converter station, and proposes the equivalent inertia constant HMMC of the flexible DC MMC to the AC system as an analysis indicator. Then, the existing various inertia support controls are compared, and the support power source, support performance, parameter design, and other aspects are analyzed to obtain the equivalent inertia constant of the flexible DC system under different controls. Furthermore, this method is extended to the multi-terminal flexible DC system to obtain the total equivalent inertia that can be provided when using the energy of multiple MMC capacitors. Finally, the effectiveness of the proposed quantitative analysis method and the support characteristics of different controls and different numbers of terminals are verified through simulation.

2. QUANTITATIVE ANALYSIS METHOD OF EQUIVALENT INERTIA CONSTANT OF SINGLE MMC

In the existing research, when using capacitor energy to support the inertia of AC power grid, it is generally believed that its support capacity can be compared to the definition of the inertia constant of synchronous motor, and the MMC energy storage time constant TE, which is used to measure it [21]. However, in fact, the response mode and speed of MMC to system frequency are different from those of synchronous motor. Under this definition, the inertia support capacity of MMC is overly limited. This section will derive the quantitative expression of MMC inertia constant from the frequency response model of MMC to AC system. Figure 1 shows the single MMC grid-connected system studied in this paper. In Figure 1: ΔP_L is the per-unit value of AC system load disturbance; ΔP_{SG} is the per-unit value of active output change of synchronous motor in primary frequency modulation process; ΔP MMC is the per-unit value of support power provided by MMC when system load is disturbed; the base values of the above power items are all the rated capacity of synchronous motor in the power grid.

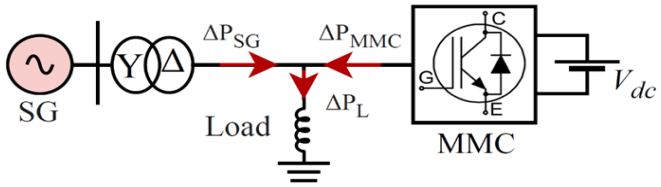

Figure 1. Schematic diagram of receiving-end AC power grid

For a receiving-end power grid, its frequency response model can be represented by Figure 2. In Figure 2: Δf_{pu} is the per-unit value of frequency change, and its base value is the power frequency 50 Hz; HSG is the equivalent inertia constant of the synchronous motor; D is the load damping response coefficient; RSG is the droop coefficient of the synchronous motor governor; TG is the governor time constant; FHP, TCH, TRH are the main parameters in the reheat turbine, representing the high-pressure cylinder work proportional coefficient, the prime mover time constant and the reheater time constant respectively.

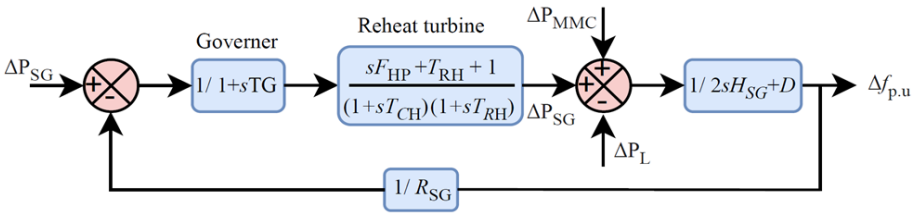

Figure 2. Frequency response model of AC system

Under normal control, the MMC sends constant power to the AC system, and $\Delta P_{MMC} = 0$ in the figure. According to the relationship in the figure, the frequency response of the system is:

$$2H_{\mathrm{SG}}\frac{\mathrm{d}\Delta f_{\mathrm{pu}}}{\mathrm{d}t} + D\Delta f_{\mathrm{pu}} = \Delta P_{\mathrm{SG}} - \Delta P_{\mathrm{L}} \tag{1}$$

when the load disturbance ΔP_{L} just occurs, since the frequency deviation is very small and there is a dead zone in the primary frequency modulation of the synchronous motor, ΔP_{SG} in (1) is approximately zero. At this time, the system frequency change in Figure 1 is only affected by ΔP_{L} let the transfer function of the reheat turbine be G(s), and the system frequency change rate at time zero can be calculated as (2).

$$\left.\frac{\mathrm{d}\Delta f_{\mathrm{pu}}}{\mathrm{d}t}\right|_{0^+} = \lim_{s\to\infty}\frac{sR_{\mathrm{SG}}(1+sT_{\mathrm{G}})}{2H_{\mathrm{SG}}R_{\mathrm{SG}}s(1+sT_{\mathrm{G}})+G(s)}\Delta P_{\mathrm{L}} = \frac{\Delta P_{\mathrm{L}}}{2H_{\mathrm{SG}}} \tag{2}$$

That is, in conventional control, the calculation for the system equivalent inertia constant is given by (3).

$$H_{\mathrm{SG}} = \frac{\Delta P_{\mathrm{L}}}{2\left.\frac{\mathrm{d}\Delta f}{\mathrm{d}t}\right|_{0^\circ}} = \frac{\Delta P_{\mathrm{L}}}{2C_0} \tag{3}$$

Where C_0 is the maximum value of the frequency per unit value change rate, which can also be considered as the frequency change rate when the load disturbance just occurs.

If MMC can support the inertia of the AC system during load disturbance, the frequency response model after considering MMC support can be represented by Figure 3 [25]. In Figure 3: HMMC is the equivalent inertia constant of MMC to the AC system. Referring to the inertia constant expression of the generator (3), HMMC is defined as half of the supporting power provided by MMC to the AC system under the unit frequency change rate.

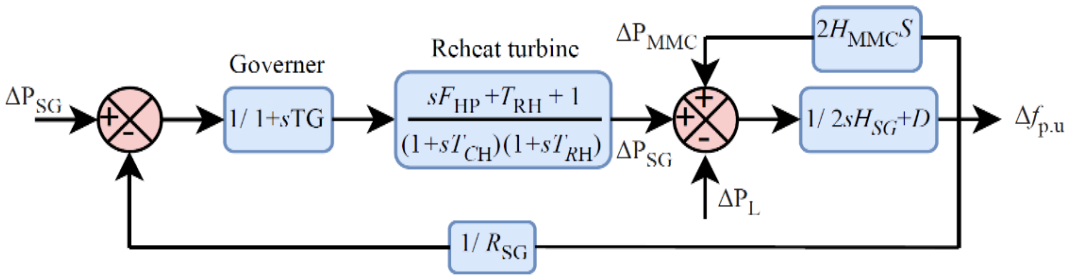

Figure 3. Frequency response model of AC system with MMC inertia response

In this model, ΔP MMC is not zero, and its size is determined by H_{MMC}. According to Figure 3, the frequency response model of the flexible DC transmission system can be expressed as (4).

$$2H_{\mathrm{SG}}\frac{\mathrm{d}\Delta f_{\mathrm{pu}}}{\mathrm{d}t}+D\Delta f_{\mathrm{pu}}=\Delta P_{\mathrm{SG}}+\Delta P_{\mathrm{MMC}}-\Delta P_{\mathrm{L}} \tag{4}$$

ΔP_{MMC} is the inertia support power provided by the converter station. Its response should be similar to that of the synchronous motor and can be expressed as (5).

$$\Delta P_{\mathrm{MMC}}=-2H_{\mathrm{MMC}}\frac{\mathrm{d}\Delta f_{\mathrm{pu}}}{\mathrm{d}t} \tag{5}$$

Under the same load disturbance, the system frequency change rate at time zero can be calculated as (6).

$$\left.\frac{\mathrm{d}\Delta f_{\mathrm{pu}}}{\mathrm{d}t}\right|_{0^{*}}=\lim_{\to\to\infty}\frac{sR_{\mathrm{SG}}(1+sT_{\mathrm{G}})}{2(H_{\mathrm{SG}}+H_{\mathrm{MMC}})R_{\mathrm{SG}}s(1+sT_{\mathrm{G}})+G(s)}\Delta P_{\mathrm{L}}=\frac{\Delta P_{\mathrm{L}}}{2(H_{\mathrm{SG}}+H_{\mathrm{MMC}})} \tag{6}$$

Analogously to (3), the total inertia constant of the system can be calculated as (7).

$$H_{\mathrm{total}}=\frac{\Delta P_{\mathrm{L}}}{2C_0}=H_{\mathrm{SG}}+H_{\mathrm{MMC}} \tag{7}$$

Where H_{total} is the total inertia constant of the AC system. From (7), we can see that after the load disturbance occurs, the inertia constant: H_{total} that the system can provide consists of two parts: one is the inertia constant of the synchronous motor itself; the other is the equivalent inertia constant provided by the MMC.

When the inertial support power ΔP_{MMC} borne by the MMC is completely provided by the submodule capacitor energy storage, the energy relationship can be expressed as (8).

$$\Delta P_{\mathrm{MMC}}=-\frac{W_0}{S_{\mathrm{SG}}}\frac{\mathrm{d}\Delta W_{\mathrm{MMc.pu}}}{\mathrm{d}t} \tag{8}$$

Where S_{SG} is the rated capacity of the synchronous motor in the power grid; $\Delta W_{\mathrm{MMc.pu}}$ is the per unit value of the MMC capacitor energy change; W_0 is the capacitor energy under rated conditions, which is also the calculation base value of $\Delta W_{\mathrm{MMc.pu}}$.

Combine (5) and (8), integrate both sides of the equation, and assume that the initial value of each physical quantity at time zero is equal to its rated value, and we can get (9).

$$\frac{W_0}{S_{\mathrm{SG}}}\Delta W_{\mathrm{MMC.pu}}=2H_{\mathrm{MMc}}\Delta f_{\mathrm{pu}} \tag{9}$$

Therefore, the equivalent inertia constant of MMC is expressed as (10).

$$H_{\mathrm{MMC}} = \frac{W_0}{2S_{\mathrm{SG}}} \frac{\Delta W_{\mathrm{MMC.pu}}}{\Delta f_{\mathrm{pu}}} \tag{10}$$

The capacitor energy W_0 at the rated state of MMC is expressed by the energy storage time constant $T_{E,MMC}$ [17] and substituted into (10) to obtain:

$$H_{\mathrm{MMC}} = \frac{T_{\mathrm{E,MMC}}}{2} \frac{S_{\mathrm{MMC}}}{S_{\mathrm{SG}}} \frac{\Delta W_{\mathrm{MMC,pu}}}{\Delta f_{\mathrm{pu}}} \tag{11}$$

Where S_{MMC} is the rated capacity of the flexible DC converter station.

It can be seen from (11) that the equivalent inertia constant of MMC for AC system is not only related to $T_{E,MMC}$, but also affected by the capacity proportion of MMC in AC system and the ratio of capacitor energy to frequency change (energy-frequency ratio). The capacity proportion reflects the actual effect of the charging and discharging process of the capacitor on the AC system, and the energy-frequency ratio is related to the control strategy of the MMC converter station, which will be discussed in detail later. The MMC equivalent inertia constant H_{MMC} obtained by considering various factors such as capacity proportion and control strategy can better reflect the actual inertia support capacity of the converter station for the AC system than $T_{E,MMC}$.

2.1. Analysis of inertia support capacity of MMC system under different control

2.1.1. Sudden increase in AC system load

As mentioned in section 2, the equivalent inertia constant HMMC of MMC is affected by the energy-frequency ratio, which is determined by the control strategy of MMC. This paper will discuss the energy-frequency ratio under different control strategies in detail and analyze the equivalent inertia constant HMMC of different controls. Figure 4 shows the schematic diagram of VSG control [14], which is one of the most common inertia support controls. Its control principle can be expressed as (12).

$$P_0 - P_{\mathrm{ref}} = 2H_{\mathrm{ctrl}} \frac{\mathrm{d}f_{\mathrm{pu}}}{\mathrm{d}t} + D\Delta f_{\mathrm{pu}} \tag{12}$$

Where: P_0 is the rated power of the AC side; P_{ref} is the actual output per unit value of the AC side, and its base value is the rated capacity of the MMC; H_{ctrl} is the inertia constant in the control.

From (12), it can be seen that the control principle is very similar to the synchronous motor rotor motion equation. Due to the addition of the damping link D, the control can not only support the system inertia, but also raise the lowest frequency point and the steady-state value after fluctuation, and has a strong supporting capacity. However, VSG control fails to indicate the source of the supporting power. Taking the receiving-end support as an example, the literatures Cardozo *et al.* and Ma *et al*. [27], [28]. point out that under this control, the supporting power provided by the MMC mostly comes from the sending-end AC system, rather than the MMC's own capacitor energy storage, so the inertial supporting capacity of the MMC cannot be quantitatively determined. At the same time, VSG control will cause the sending-end AC system to fluctuate in frequency due to changes in the synchronous motor output, thereby affecting the operating stability of the sending-end power grid.

To overcome the above problems, Figures 5 and 6 show two control strategies that can use MMC capacitor energy to support the power grid. Under these strategies, the load disturbance of the receiving-end power grid will not affect the frequency stability of the sending-end power grid, and the support potential of MMC itself can be brought into play.

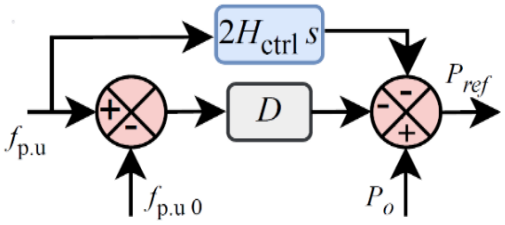

Figure 4. Schematic diagram of VSG control

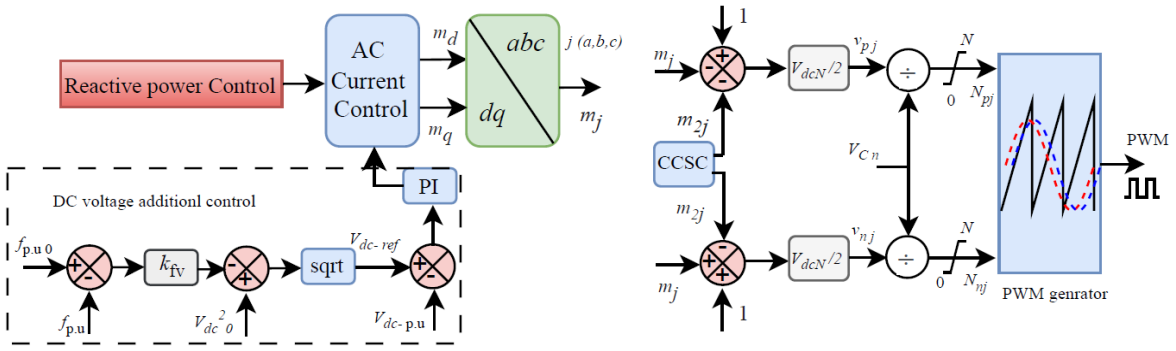

Figure 5. Schematic diagram of INEC strategy

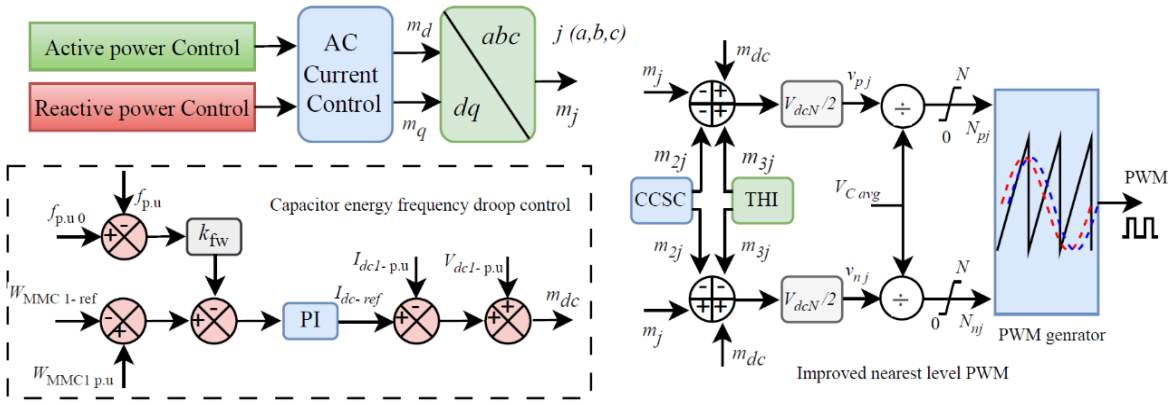

Figure 6. Four-dimensional control of MMC

Figure 5 shows an MMC inertia emulation control (INEC) proposed in the Zhu *et al.* [18]. Its principle is to add additional control of DC voltage on the basis of double closed-loop vector control, and use the coupling characteristics of DC voltage and capacitor voltage to release/absorb capacitor energy by changing DC voltage, thereby simulating the inertia link of the synchronous motor. According to Figure 5, we can get (13).

$$V_{\mathrm{dc,pu}} = \sqrt{V_{\mathrm{dc,puv}}^2 + k_{\mathrm{fv}}\Delta f_{\mathrm{pu}}} \tag{13}$$

Where $V_{\mathrm{dc,pu}}$ is the per unit value of the DC voltage of the converter station; under rated conditions, and its value is 1; k_{fv} is the droop control gain.

Considering that in the per-unit system, the MMC energy $\Delta W_{\mathrm{MMC.pu}}$ is the square of the DC voltage $V_{\mathrm{dc,pu}}$, the relationship between energy and frequency change when the INEC strategy is adopted is:

$$\Delta W_{\mathrm{MMC,pu}} = V_{\mathrm{dc,pu}}^2 - V_{\mathrm{dc,pu0}}^2 = k_{\mathrm{fv}}\Delta f_{\mathrm{pu}} \tag{14}$$

from (14), we can see that the energy frequency ratio under the INEC strategy is the droop coefficient k_{fv}. Substituting (14) into (11), we can get the inertia constant under the INEC strategy as given by (15).

$$H_{\mathrm{MMC}} = \frac{T_{\mathrm{E,MMC}}}{2}\frac{S_{\mathrm{MMC}}}{S_{\mathrm{SG}}}k_{\mathrm{fv}} \tag{15}$$

The selection of droop control gain k_{fv} is determined by the system DC voltage limit per unit value $V_{\mathrm{dc,pu\,lim}}$ and the AC system frequency deviation limit per unit value $\Delta f_{\mathrm{pu}}lim$, which can be expressed as (16).

$$k_{\mathrm{fv}}=\frac{V_{\mathrm{dc,pu,\,lim}}^{2}-V_{\mathrm{dc,pu0}}^{2}}{\Delta f_{\mathrm{pu,lim}}} \tag{16}$$

According to Zhang *et al.* [24], the frequency deviation limit is generally considered to be ±0.5 Hz, that is, 0.01 p.u. According to Jovcic [29], the DC voltage of the converter station can be operated to Mac $V_{\mathrm{dc}n}$ at the lowest, where Mac is the AC modulation ratio, and its value is generally 0.85~0.95, and $V_{\mathrm{dc}n}$ is the rated DC voltage, that is, the DC voltage can be as low as 0.85 p.u. The upper limit of the DC voltage operation generally does not exceed 1.10 p.u. [30]. Therefore, the DC voltage deviation limit $V_{\mathrm{dc,pu\,lim}}$= [0.85, 1.10] p.u. From (15) and (16), it can be seen that the DC/capacitor voltage deviation limit of the dual closed-loop vector control determines the gain coefficient k_{fv} of the INEC strategy, and its value directly affects the equivalent inertia constant of the flexible DC MMC. Assuming the energy storage time constant $T_{E,MMC}$ is 40 ms, taking an AC system consisting of a 1000 MW/±500 kV MMC and a 2000 MW synchronous motor as an example, substituting the parameters into (15) and (16), it can be calculated that the inertia constant HMMC that the INEC strategy can provide is 0.28 s and 0.21 s respectively when the load suddenly increases/decreases.

Figure 6 shows the MMC four-dimensional control scheme proposed in Zhang *et al.* [24]. The DC modulation ratio M_{dc} enables the control to control the DC voltage and AC voltage separately, while the improved nearest level modulation strategy uses the variable capacitor voltage V_{C_avg} to replace the capacitor voltage rating under the traditional scheme, so that the DC line voltage and the submodule capacitor voltage are mathematically decoupled.

At the same time, by using the frequency-capacitance energy (f-W) droop control in the red dashed box of Figure 6, the submodule capacitance energy can be changed proportionally with the frequency fluctuation, so that it has an inertia support capacity similar to that of a synchronous motor. Therefore, when the f-W droop control strategy is adopted, the inertia constant that the MMC energy can provide can be expressed as (17).

$$H_{\mathrm{MMC}}=\frac{T_{\mathrm{E,MMC}}}{2}\frac{S_{\mathrm{MMC}}}{S_{\mathrm{SG}}}k_{\mathrm{fw}} \tag{17}$$

Where k_{fw} is the droop coefficient in control, that is, the energy-frequency ratio. The selection of k_{fw} is determined by the MMC capacitor energy utilization limit per unit value $W_{\mathrm{pu\,lim}}$ and the AC system frequency deviation limit per unit value $\Delta f_{\mathrm{pu,lim}}$ which can be expressed as (18).

$$k_{\mathrm{fw}}=\frac{W_{\mathrm{pu,lim}}-W_{\mathrm{pu0}}}{\Delta f_{\mathrm{pu,lim}}} \tag{18}$$

Where: W_{pu0} is the per unit value of the capacitance energy of the MMC under rated conditions, and its value is 1. According to the Zhang *et al.* [24], the variation range of the capacitor voltage per unit value under four-dimensional control is $V_{C_{avg},pu,lim}$ = [0.768, 1.500] p.u., that is, the variation range of the capacitor energy is $W_{\mathrm{pu\,lim}}$ = [0.59, 2.25] p.u. From (17) and (18), it can be seen that the capacitor voltage/energy deviation limit of the MMC four-dimensional control determines the droop coefficient k_{fw} of the f-W droop control, and its value directly affects the equivalent inertia constant of the flexible DC MMC. Using the same test system as the INEC strategy, it can be calculated that the inertia constant H_{MMC} provided by the MMC energy when the f-W droop control is adopted is 0.41 s and 1.25 s respectively when the load increases/decreases suddenly.

Based on the above discussion, the equivalent inertia constant of the flexible DC transmission system is compared between the f-W droop control using four-dimensional control and the INEC strategy using double closed-loop vector control when the load increases/decreases suddenly, as shown in Table 1. It can be seen from Table 1 that for the same system working condition, compared with the INEC strategy, under the f-W droop control based on four-dimensional control, the equivalent inertia constant H of MMC is larger and the inertia support capacity is stronger.

Table 1. Comparison of MMC equivalent inertia constants under different control strategies

Control strategy	Hmm/s	
	Load increasing	Load reduction
INEC	0.28	0.21
f-W droop control	0.41	1.25
Control strategy	Hmm/s	

2.2. Comparative analysis of equivalent inertia constant and existing indicators

In order to quantitatively analyze the MMC's ability to support grid inertia, existing studies have proposed a variety of inertia quantification indicators. This section compares the proposed MMC equivalent inertia constant with existing studies to verify the advantages and completeness of the indicators proposed in this paper. Yang *et al.* [25] defines an MMC inertia constant that takes into account the proportion of new energy penetration. Assume that the rotor kinetic energy of the synchronous motor is $0.5\,j\omega^2$, and the capacitor energy storage in the MMC is $0.5\,CV_C^2$, where j is the moment of inertia, ω is the speed of the synchronous motor, and C is the size of the MMC capacitor. Yang *et al.* [25] equates the two and makes the capacitor voltage V_C change proportionally with the speed of the synchronous motor (grid frequency) to simulate the inertia response of the synchronous motor. Assume that the system allows a maximum frequency deviation limit $\Delta f_{\mathrm{lim}} = \lambda f_o$, and the maximum capacitor voltage deviation $\Delta V_{\mathrm{C\,lim}}$ satisfies $\Delta V_{\mathrm{C\,lim}}$with the rated capacitor voltage $\Delta V_{\mathrm{C\,lim}} = \beta V_{\mathrm{C0}}$, where λ and β are corresponding proportional coefficients. Then the MMC capacitor voltage change command value ΔV_{C}^* and the frequency deviation Δf should satisfy.

$$\Delta V_{\mathrm{C}}^* = \frac{\beta}{\lambda} V_{\mathrm{C0}} \Delta f \tag{19}$$

Define the total grid capacity $S_{\mathrm{Grid}} = S_{\mathrm{MMC}} + S_{\mathrm{SG}}$, then the MMC inertia constant H_{MMC1} defined in the Zhu *et al.* [18] is given by (20).

$$H_{MMC1} = \frac{W_o \quad \beta}{S_{Grid} \ \lambda} \tag{20}$$

From Section 2.1.1, we know that the frequency deviation limit is 0.01 p.u., that is, λ = 0.01. When MMC adopts four-dimensional control, the per-unit value variation range of capacitor voltage $V_{C.pu,\ lim}$ = [0.768, 1.500] p.u., that is, β is 0.232 and 0.500, respectively, when the load increases/decreases suddenly. Taking the flexible DC transmission system parameters described in Section 2.1.1 as an example, the MMC inertia constant H_{MMC1} under this definition can be calculated to be 0.31 s and 0.67 s, respectively, when the load increases/decreases suddenly.

From the above analysis, it can be seen that the H_{MMC1} defined in the Zhang *at al*. [23] under the same control is smaller than the flexible DC equivalent inertia constant defined in this paper. The main reasons are as follows:

i) The power base value selected in the calculation of Yang *et al*. [25] is S_{Grid}. Singh *et al.* [8] points out that when the access of new energy sources increases, if the number of synchronous motors in the grid remains unchanged and the kinetic energy remains unchanged, the rate of change of system frequency under the same disturbance power remains unchanged. There is no equivalent relationship between the inertia constant calculated by the above method and the system frequency. This paper uses the capacity of the synchronous motor of the grid S_{SG} as the base value for power calculation, which can better reflect the actual impact of capacitor energy on the AC system.
ii) In Zhu *et al.* [18], the capacitor voltage V_{C} is proportional to the system frequency, which is inconsistent with the physical meaning of the inertia constant. The MMC inertia constant is defined as half of the power supported by the MMC for the AC system under the unit frequency change rate, that is, the system frequency should be proportional to the capacitor energy.

Kim *et al.* [26] compared the MMC capacitor energy storage to the kinetic energy of the synchronous motor rotor and proposed the flexible DC inertia constant HMMC2. Assuming the rated speed of the synchronous motor is ω_o, its rotor kinetic energy ω_k can be expressed as (21).

$$\omega_k = 0.5 j\omega^2 \tag{21}$$

Assuming the maximum allowable speed (frequency) deviation is ω_{lim}, when load disturbance occurs, the energy limit $\Delta W_{k,lim}$ injected by the synchronous motor to support the AC power grid can be expressed as (22).

$$\Delta W_{k,lim} = \frac{J(\omega_o^2 - \omega_{lim}^2)}{2} = \left(1 - \Delta f_{pu.lim}^2\right) \frac{J}{2} \omega_o^2 = W_k \, K_f \tag{22}$$

Where k_f is the ratio between the kinetic energy change limit and the rated kinetic energy. Kim *et al.* [26] combined the DC voltage deviation limit and the third harmonic injection effect to obtain that the bridge arm

can be put into use up to 1.265 N submodules, where N is the number of submodules put into use under the rated state of the MMC. Then the capacitance energy change limit ΔW_{lim} can be calculated as (23).

$$\Delta W_{lim} = \left(1 - \frac{1}{1.265^2}\right) W_o \approx 0.375\ W_o \tag{23}$$

Combining (22) and (23), let the MMC capacitor energy change limit ΔW_{lim} be equal to the analog synchronous motor rotor kinetic energy change limit $\Delta W_{k,lim}$, and the flexible DC inertia constant H_{MMC2} defined in Zhu *et al.* [19] is obtained as (24).

$$H_{MMC2} = \frac{0.375\ W_o}{S_{SG}\ \ k_f} \tag{24}$$

Taking the above-mentioned flexible DC transmission system parameters as an example, the HMMC2 defined in the literature can be calculated to be 0.375 s when the load suddenly increases. Similarly, HMMC2 under the load suddenly decrease condition is also 0.375 s, both of which are smaller than the equivalent inertia constant of the flexible DC under the four-dimensional control proposed in this paper. The main reason is that Kim *et al.* [26] did not fully analyze the energy utilization limit of the MMC submodule capacitor after the DC voltage and capacitor voltage were decoupled, and did not consider the changes in the inertia support capacity caused by the different energy absorption and release ranges of the capacitor.

The inertia constants defined in Zhu *et al.* [18], [19] and the MMC equivalent inertia constants proposed in this paper are compared, as shown in Table 2. From the above discussion, it can be seen that the flexible DC equivalent inertia constant HMMC proposed in this paper not only considers the actual effect of capacitor energy storage on the AC system, but also covers the differences in energy utilization range under different control and different load disturbance conditions, and can accurately quantify the inertia support capacity of MMC.

Table 2. Comparison of HMMC, HMMC1 [18], and HMMC2 [19]

Working conditions	HMMC/s proposed	HMMC1/s	HMMC2/s
Load surge	0.41	0.31	0.375
Load reduction	1.25	0.67	0.375

3. ANALYSIS OF THE INERTIA SUPPORT CAPABILITY OF MULTI-TERMINAL MMC FOR RECEIVING END

As can be seen from section 2, MMC four-dimensional control can maximize the use of sub-module capacitor energy to provide inertia support for the AC system without affecting the power stability of other AC systems. This chapter will take four-dimensional control as an example to discuss the inertia support law of the multi-terminal modular multi-level direct current (MMC-MTDC) system.

In section 1 and 2, the inertia support capacity of a single MMC converter station for the AC system was calculated. For a two-terminal system, if the capacitor energy in two MMCs can be used to support the receiving-end grid at the same time, it can be seen from (11) that its support capacity is obviously twice that of a single converter station.

The research object is extended to the three-terminal MMC-MTDC system. Take the system with one transmission and two receptions shown in Figure 7 as an example for discussion. In the figure: the transmission end MMC1 is 2000 MW, the reception end MMC2 and MMC3 are 1000 MW respectively, and all MMCs have the same energy storage time constant, which is TE, MMC=40 ms. In the AC system connected to MMC2, the synchronous motor capacity S_{SG2} is 2000 MW. The inertia support law of the multi-terminal system for the AC system connected to the reception end MMC2 is discussed.

When only the directly connected MMC2 supports the system frequency, its supporting capacity is the same as that of the single 1000 MW MMC in section 2. As shown in Table 1, the equivalent inertia constant H of the single MMC converter station is 0.41 s and 1.25 s respectively when the load increases/decreases. Considering that MMC3 also participates in the support, and assuming that MMC3 and MMC2 have the same energy-frequency ratio k_{fw}, the total energy of the capacitors participating in the frequency support in the system becomes twice that of the single MMC support, and the equivalent inertia constant of the system also becomes twice that of the single MMC support. Therefore, when the load increases/decreases suddenly, the equivalent inertia constant HMMC of the flexible DC transmission system is 0.82 s and 2.50 s, respectively.

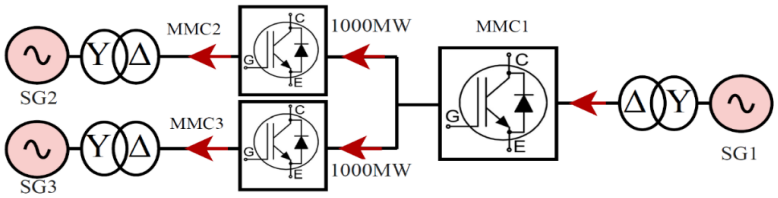

Figure 7. Schematic diagram of a three-terminal MMC system

If the capacitive energy of the 2000 MW MMC1 at the sending end can also respond to the inertia of the AC system connected to the receiving end MMC2, the support capacity of the system will be further improved. Assuming that MMC1 has the same energy frequency ratio k_{fw} as other MMCs, since the capacity of MMC1 is twice that of MMC2, the equivalent inertia constant provided by MMC1 is twice that of MMC2, that is, the inertia constant provided when the load increases/decreases suddenly is 0.82 s and 2.50 s respectively. Considering the capacitive energy of all MMCs in the flexible DC system, the overall HMMC of the system is 1.64 s and 5.00 s respectively. In summary, for an MMC-MTDC system, if the capacitor energy of all converter stations can be used for the inertia support of the receiving system at the same time, under the same energy storage time constant $T_{\mathrm{E,MMC}}$ and energy frequency ratio k_{fw}, the inertia support capacity of the MMC-MTDC system is determined by the total capacity of the system. The equivalent inertia constant HMMC, tot of the MMC-MTDC system can be expressed as (25).

$$H_{\mathrm{MMC,tot}} = T_{\mathrm{E.MMC,tot}} \frac{S_{\mathrm{MMC,tot}}}{S_{\mathrm{GD,d}}} \frac{\Delta W_{MMC,pu}}{\Delta f_{pu}} \tag{25}$$

Where $S_{\mathrm{MMC,tot}}$ is the rated capacity of the MMC-MTDC system and $S_{\mathrm{SG,d}}$ is the rated capacity of the synchronous motor of the AC system with load disturbance.

When the three-terminal MMC-MTDC system adopts the INEC strategy, due to the coupling relationship between the DC voltage and the capacitor voltage, the change of the DC voltage will affect the three converter station capacitors to release/absorb energy to support the AC grid on the disturbance side. According to the discussion in section 2, compared with the four-dimensional control, the INEC strategy only changes the energy-frequency ratio. Substituting the energy-frequency ratio under this strategy into (25), the theoretical equivalent inertia constant of the three-terminal system under the INEC strategy can be calculated to be 1.1 s and 0.84 s when the load increases/decreases. The comparison with the H_{MMC} of f-W droop control is shown in Table 3. It can be seen from Table 3 that when adopting f-W droop control, the equivalent inertia constant of the three-terminal MMC-MTDC system under different working conditions is large, and the frequency support capability of the power grid is strong.

Table 3. Comparison of HMMC of three-terminal MMC-MTDC system under different control strategies

Control strategy	Hmm/s	
	Load increasing	Load reduction
INEC	1.10	0.84
f-W droop control	1.64	5.00

When the AC grid connected to MMC_2 is disturbed, in order to ensure that the capacitor energy of MMC_1 and MMC_3 can flow to MMC_2, MMC_1, and MMC_3 can be controlled by constant AC power. According to the power balance, the power generated by absorbing/releasing energy through the converter station capacitor can only flow to the AC system connected to MMC2 through the DC line. For two typical three-terminal MMC-MTDC system topologies, the flow of the supporting power provided by the capacitor energy in the flexible DC transmission system is shown in Figure 8.

Since MMC1 and MMC3, except MMC2, cannot directly obtain the frequency change when the load disturbance occurs, in order to enable each converter station to accurately release energy to support the receiving end system, the scheme proposed in Singh *et al.* [8] can be used to make the DC voltage reflect the frequency change through frequency-DC voltage droop control. The DC voltage can also be changed by simulating inertia, as proposed in [30], and then the receiving end equivalent frequency feq is obtained through frequency reduction control, and feq is added to the outer loop of f-W droop control to make the capacitor release energy. The specific control details are not the main object of this paper and will not be introduced in detail here.

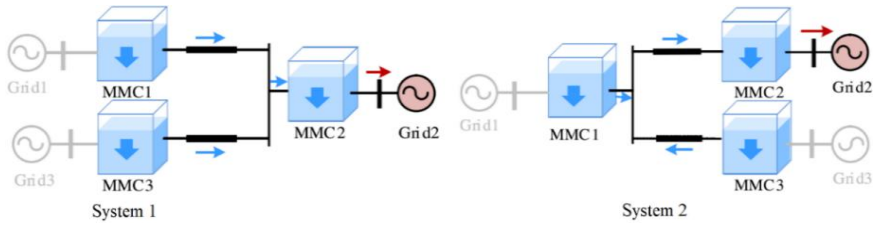

Figure 8. Support power flow of a three-terminal MMC system

4. SIMULATION VERIFICATION

In order to verify the effectiveness of the quantitative analysis method of MMC inertia support capacity proposed in this paper, and to compare the effects of different numbers of support terminals and different control strategies, a three-terminal MMC-MTDC system as shown in Figure 8 was built based on PSCAD/EMTDC, and a load disturbance was applied to the AC power grid connected to MMC2 for verification. The MMC-MTDC system adopts a master-slave control strategy, in which MMC2 adopts constant DC voltage control, and a frequency droop link is added to the DC voltage outer loop to reflect the frequency change of the receiving end system. Taking the f-W droop control under four-dimensional control as an example, its specific control scheme is shown in Figure 9. MMC1 and MMC3 adopt constant power control and additional frequency restoration control to enable them to obtain the frequency information of the AC system on the MMC2 side [8]. The specific control method and frequency restoration strategy (taking MMC1 as an example) are shown in Figures 10 and 11. The synchronous motor capacity of the AC system where the three converter stations are located is 2000 MW, and the inertia constant HSG = 4.5 s. The receiving end system connected to MMC2 initially carries 2000 MW, and a 5% load mutation (±100 MW) occurs at 13 s. The specific parameters of the three-terminal MTDC system are shown in Table 4.

When the three MMC converter stations adopt the INEC strategy and f-W droop control, the droop coefficient gains k_{fv} and k_{fw} in the two controls are designed using (16) and (18) respectively. When the INEC strategy is adopted, since it is based on two-dimensional control, the capacitance energy of the three-terminal MMC will be used simultaneously when participating in inertia support. When VSG control is adopted, the parameters of MMC2 and MMC3 are shown in Table 5. Under four-dimensional control, the effects of using the capacitance energy of MMC2 single-terminal, MMC3+MMC2 two-terminal, and MMC1+MMC2+MMC3 three-terminal converter stations to participate in inertia support are simulated to verify the support characteristics of different controls and different numbers of terminals mentioned above.

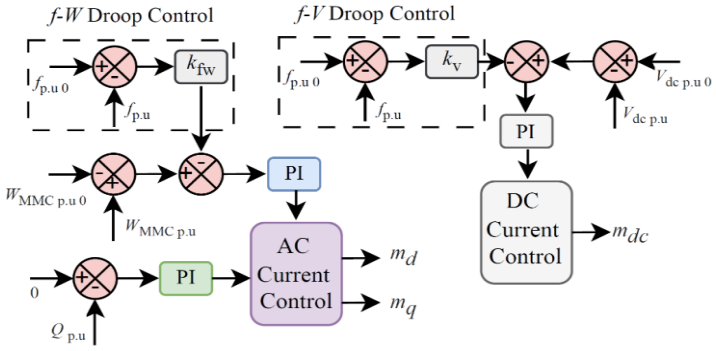

Figure 9. Schematic diagram of MMC constant DC voltage control (MMC2)

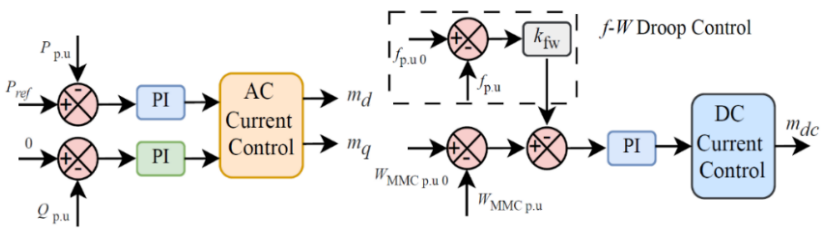

Figure 10. Schematic diagram of MMC constant power control (MMC1 and MMC3)

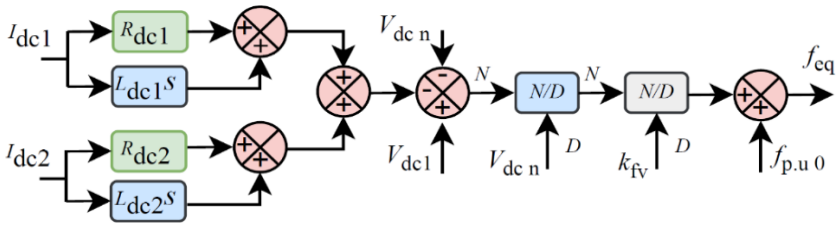

Figure 11. Schematic diagram of frequency reduction control (MMC1)

Table 4. Main parameter setting of MMC-MTDC system

MMC	Rated power MW	Rated DC voltage KV	Rated AC voltage KV	arm inductance	Submodule number	Submodule capacitance	Submodule rated voltage
MMC1	2000	±500	330	0.267 H	400	10.67 mf	2.5 kV
MMC2	1000	±500	330	0.134 H	400	5.33 mf	2.5 kV
MMC3	1000	±500	330	0.134 H	400	5.33 mf	2.5 kV

Table 5. Design of VSG control parameters for three-terminal MMC-MTDC system

Converter Station	Damping coefficient D	Inertia coefficient H_{ctrl}
MMC1	5	0.82 s
MMC3	10	1.64 s

4.1. Case 1: Sudden increase in AC system load

When t = 13 s, the load of the AC system connected to the converter station MMC2 suddenly increases by 100 MW. The simulation results under different numbers of support terminals and different strategies are shown in Figure 12. As shown in Figure 12(a), under VSG control, the load disturbance on the MMC2 side of the flexible DC system will affect the frequency of the AC system connected to the converter station MMC3, and its change trend is similar to the sudden increase in system load. However, when the INEC strategy and four-dimensional control that fully utilizes capacitor energy for support are adopted, the AC system at MMC3 will not be affected. At this time, the supporting power comes entirely from the capacitor energy storage inside the flexible DC transmission system. As shown in Figure 12(a), under VSG control, the load disturbance on the MMC2 side of the flexible DC system will affect the frequency of the AC system connected to the converter station MMC3, and its change trend is similar to the sudden increase in system load. However, when the INEC strategy and four-dimensional control that fully utilizes capacitor energy for support are adopted, the AC system at MMC3 will not be affected. At this time, the supporting power comes entirely from the capacitor energy storage inside the flexible DC transmission system. When the load suddenly increases by 100 MW (5%), according to (17), the equivalent inertia constant H of a single MMC under f-W droop control is 0.41 s. As shown in Figure 12(b), when only MMC2 participates in the support, the frequency change rate C_O of the system increases from -0.275 Hz/s without MMC support to -0.253 Hz/s. According to (3) and (7), the inertia constant HSG of the synchronous motor at the initial moment is 4.54 s and the total inertia constant Htotal of the system after single MMC capacitor energy support is 4.94 s. It can be seen that when MMC2 participates in the inertia support, the inertia constant of the system increases by about the difference between Htotal and HSG, that is, 0.4 s, which is close to the theoretical calculation results in Table 3, verifying the correctness of the proposed inertia support calculation. As shown in Figure 12(c), when the capacitor energies of MMC2 and MMC3 are supported at the same time, C_O can be increased to -0.233 Hz/s. It can be calculated that the Htotal of the system is 5.36 s, that is, the total inertia constant of the AC system is increased by about 0.82 s, which is twice that of the single MMC2 support. When the 2000 MW MMC1 capacitor energy at the sending end also supports, it can be seen from Figure 12(d) that the C_O of the AC system under four-dimensional control is further raised to 0.201 Hz/s. At this time, the calculated Htotal is 6.22 s, and the equivalent inertia constant HMMC, tot of the MMC-MTDC system is 1.68 s, which is very close to the theoretical calculation result of 1.64 s in section 3, verifying the effectiveness of the inertia constant calculation method of the multi-terminal MMC-MTDC system mentioned above. Under the INEC strategy, the system's C_O is raised to 0.229 Hz/s. The equivalent inertia constant HMMC, tot of the flexible DC transmission system under this control strategy is calculated to be 0.92 s, which is less than the theoretical calculation result of 1.1 s shown in Table 3. Compared with the inertia constant of 1.64 s under four-dimensional control, the inertia support capacity is weaker because the energy utilization range of the capacitor under the INEC strategy is smaller and the energy frequency is lower.

As shown in Figure 12(e), when the number of MMC terminals supported in the multi-terminal system increases, the system frequency changes significantly more smoothly, and the lowest point also increases, which verifies that the frequency support strength of the power grid can be improved while utilizing the capacitor energy of the multi-terminal MMC-MTDC system. As shown in Figure 12(f), when the disturbance occurs, the system frequency changes most smoothly under the f-W droop control, and the inertia support effect is the best. As shown in Figure 12(g), under the f-W droop control, the MMC capacitor energy can be adjusted separately, and the system DC voltage change is mainly used to reflect the frequency fluctuation of the receiving end, and its change amplitude and rate are both smaller than the INEC strategy. As shown in Figure 12(h), under the same load disturbance, compared with the INEC strategy, the f-W droop control has less impact on the DC voltage and more full utilization of the capacitor energy. During the above support process, the AC power output of MMC2 will deviate from the rated value as the capacitor energy changes, and the rate of change determines the degree of deviation. After the support is completed, the energy recovery strategy in the literature [24] can be used to restore the MMC capacitor energy and DC voltage to the rated value. After steady state, the output power of MMC2 will also be restored to 1 p.u.

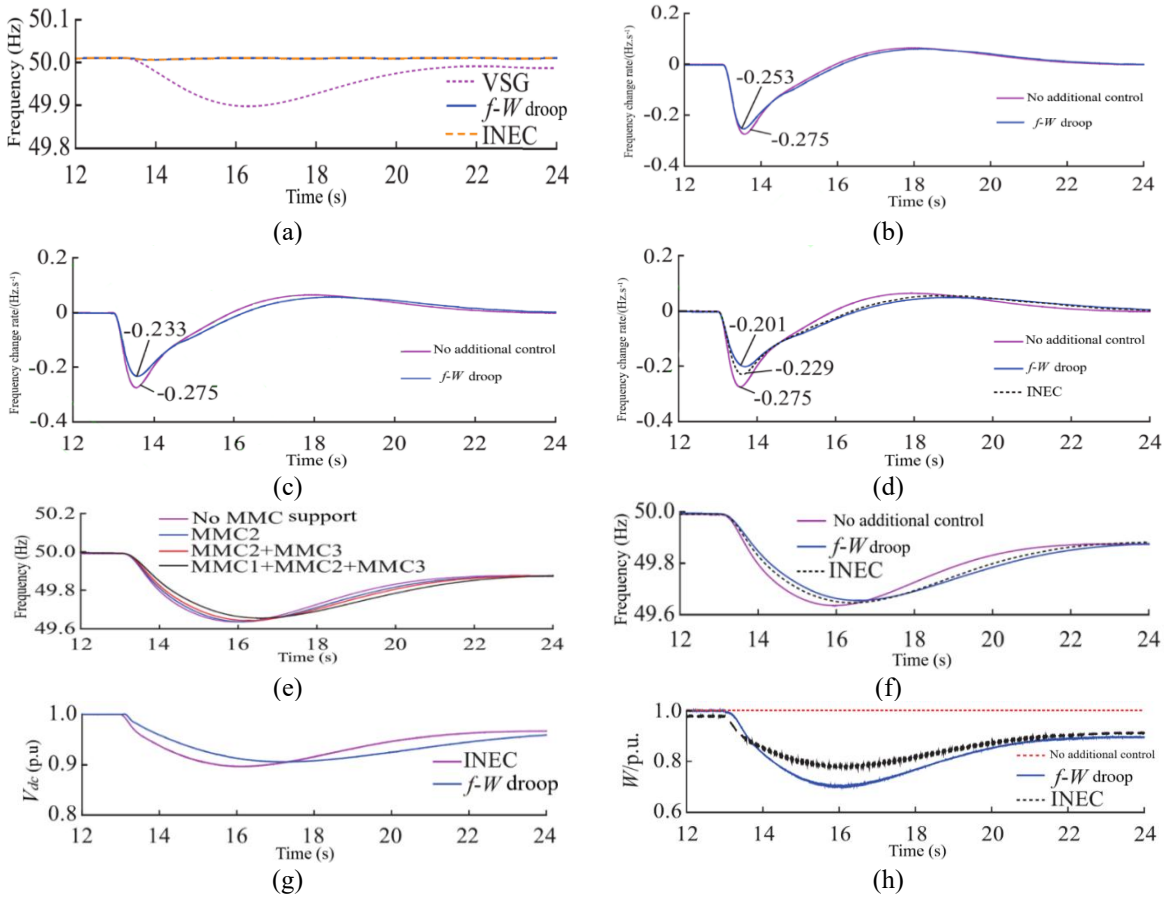

Figure 12. Simulation waveforms under a 100 MW load increase: (a) AC grid frequency, (b) frequency change rate with MMC_2 support, (c) frequency change rate with MMC_2 and MMC_3 support, (d) three-terminal MMC frequency change rate, (e) frequency response with different numbers of MMCs, (f) frequency under different control strategies, (g) DC voltage, and (h) MMC capacitor energy

4.2. Case 2: Sudden reduction of AC system load

At t = 13 s, the load of the AC system connected to the converter station MMC2 suddenly drops by 100 MW. The simulation results under different MMC support terminals and different control strategies are shown in Figure 13. When the load suddenly decreases by 100 MW, it can be seen from (17) that the theoretical inertia constant HMMC of a single MMC under this condition is 1.25 s. As shown in Figure 13(a), when only MMC2 participates in the support, the system's C_O decreases from 2.75 Hz/s when there is no MMC support to 0.221 Hz/s. It can be calculated that after the single MMC capacitor energy support,

the system's total inertia constant Htotal is 5.66 s, which is 1.12 s higher than that of HSG, and is close to the theoretical derivation result of 1.25 s. As shown in Figure 13(b), when MMC2 and MMC3 capacitor energy support at the same time, the system C_O decreases to 0.182 Hz/s, and Htotal is 6.87 s. Therefore, after MMC2 and MMC3 participate in the support, the inertia constant of the AC system increases by about 2.33 s, and the support effect is about twice that of single MMC support. As shown in Figure 13(c), when the capacitor energy of the converter station MMC1 is put into support, the system's C_O is further reduced to 0.136 Hz/s. It can be calculated that Htotal at this time is 9.19 s, that is, the equivalent inertia constant HMMC, tot of the entire three-terminal system is 4.65 s. According to (25), the theoretical calculation result of HMMC, tot is 5 s, with a small error, which verifies the effectiveness of the quantitative analysis strategy.

When the INEC strategy is adopted, C_O is reduced to 0.232 Hz/s, and the HMMC, tot under this control strategy is calculated to be 0.85 s, which is very small compared with the theoretical calculation result of 0.84 s shown in Table 3. Compared with the inertia constant of 5 s under f-W droop control, the INEC strategy has a small range of capacitor energy utilization when the load suddenly decreases, and its support effect is weak. Figure 13(d) shows the frequency change of the system under the support of MMC with different terminal numbers. With the increase of the number of supported terminals, the system frequency changes more slowly and the highest point gradually decreases. At the same time, since the absorption margin of capacitor energy is greater than its release margin, its support effect on the grid frequency is more significant. Figure 13(e) shows the frequency change of the system under different controls. The system frequency changes most smoothly under f-W droop control, and the system inertia constant is the largest at this time, while the inertia of the system under INEC strategy is smaller than that under f-W droop control. According to Figures 13(f) and 13(g), under f-W droop control, the DC voltage change can reflect the frequency fluctuation of the AC system connected to MMC2, and its change amplitude and rate are smaller than those of INEC strategy. However, since the four-dimensional control decouples the DC voltage and capacitor voltage, f-W droop control makes more full use of capacitor energy.

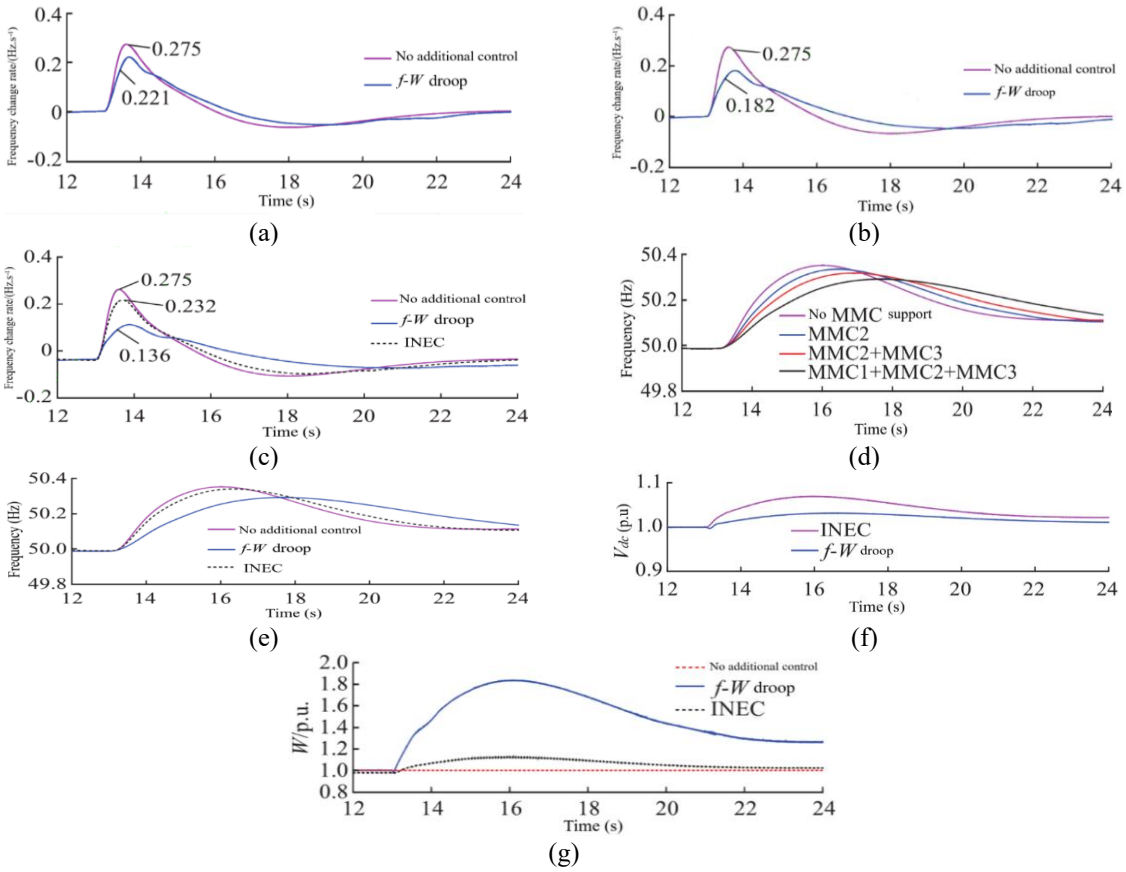

Figure 13. Simulation waveforms under a 100 MW load decrease: (a) frequency change rate with MMC$_2$ capacitor energy support, (b) frequency change rate with MMC$_2$ and MMC$_3$ capacitor energy support, (c) frequency change rate of a three-terminal MMC under different control strategies, (d) system frequency under different numbers of MMCs, (e) system frequency under different control strategies, (f) DC voltage under different control strategies, and (g) MMC capacitor energy under different control strategies

Consequently, it is evident that elevated droop gains diminish damping and may constrict stability margins, leading to oscillatory or underdamped frequency dynamics. Augmenting the virtual inertia coefficient decelerates system responsiveness and amplifies phase lag, thereby destabilising the converter-grid interaction in weak-grid scenarios. Consequently, the synchronised adjustment of droop and inertia is crucial, as high levels of either might displace dominant poles into the right-half plane, instigating oscillations in low-inertia grids.

5. CONCLUSION

This paper presents a quantitative methodology for assessing the inertia response of MMC converter stations through the equivalent inertia constant HMMC. The analysis indicated that inertia support is contingent upon the MMC energy-storage time constant, the converter–motor capacity ratio, and the energy–frequency relationship. Among the evaluated strategies, f–W droop control offers the most substantial inertia support owing to its broader energy-utilization range, whereas INEC ensures stable frequency maintenance. Conversely, VSG control conveys disturbances to undisturbed AC systems. Applying the method to MMC-MTDC systems revealed that total inertia support escalates with the cumulative converter capacity. PSCAD simulations validated these results, demonstrating that the three-terminal system attained inertia values akin to those of synchronous machines. The suggested approach provides a concise and dependable instrument for formulating inertia-support strategies in flexible DC and MTDC grids.

ACKNOWLEDGMENTS

The authors acknowledge the support of the College of Engineering, Mustansiriyah University (https://webmain.uommustansiriyah.edu.iq).

FUNDING INFORMATION

There is no funding agency that have supported this work.

AUTHOR CONTRIBUTIONS STATEMENT

This journal uses the Contributor Roles Taxonomy (CRediT) to recognize individual author contributions, reduce authorship disputes, and facilitate collaboration.

Name of Author	C	M	So	Va	Fo	I	R	D	O	E	Vi	Su	P	Fu
Dunya Sh. Wais	✓	✓	✓	✓	✓	✓		✓	✓	✓			✓	✓
Huda A. Abbood		✓	✓			✓		✓	✓	✓	✓	✓		✓

C : **C**onceptualization
M : **M**ethodology
So : **So**ftware
Va : **Va**lidation
Fo : **Fo**rmal analysis
I : **I**nvestigation
R : **R**esources
D : **D**ata Curation
O : Writing - **O**riginal Draft
E : Writing - Review & **E**diting
Vi : **Vi**sualization
Su : **Su**pervision
P : **P**roject administration
Fu : **Fu**nding acquisition

CONFLICT OF INTEREST STATEMENT

The authors declare that they have no known competing financial interests or personal relationships that could have appeared to influence the work reported in this paper.

DATA AVAILABILITY

The data that support the findings of this study are openly available in https://2u.pw/zP7uY9 at doi: https://2u.pw/qxTRnT.

REFERENCES

[1] L. Qi, M. Wang, X. Zhang, H. Shen, H. Wang, and C. Jiao, "Analysis for magnetic field disturbance of modular multilevel converter based high voltage direct current (MMC-HVDC) converter valve," *High Voltage*, vol. 8, no. 1, pp. 91–101, 2023, doi: 10.1049/hve2.12227.

[2] A. Singh, V. Jately, P. Kala, and Y. Yang, "Enhancing power quality in electric vehicles and battery energy storage systems using multilevel inverter topologies – A review," *Journal of Energy Storage*, vol. 110, 2025, doi: 10.1016/j.est.2024.115274.

[3] A. K. Hannan, Z. A. Kadhum, A. K. Ali, A. Farghly, and L. K. Hanan, "Suppression of the capacitor voltage ripple in modular multilevel converter for variable-speed drive applications," *Tikrit Journal of Engineering Sciences*, vol. 31, no. 1, pp. 56–74, 2024, doi: 10.25130/tjes.31.1.6.

[4] A. K. Hannan and T. K. Hassan, "Design and simulation of modular multilevel converter fed induction motor drive," *Indonesian Journal of Electrical Engineering and Informatics (IJEEI)*, vol. 9, no. 1, pp. 22–36, 2021, doi: 10.52549/ijeei.v9i1.2699.

[5] A. Farghly, A. Elserougi, A. Abdel-khalik, and R. Hamdy, "A hybrid mixed-cells DC-DC modular multilevel converter with balanced arm energy and DC fault blocking capability for high voltage direct current systems," *International Journal of Circuit Theory and Applications*, vol. 52, no. 9, pp. 4556–4581, 2024, doi: 10.1002/cta.3944.

[6] A. Erat and A. M. Vural, "DC/DC modular multilevel converters for HVDC interconnection: a comprehensive review," *International Transactions on Electrical Energy Systems*, vol. 2022, no. 1, pp. 1–49, Sep. 2022, doi: 10.1155/2022/2687243.

[7] H. A. Hasan, A. K. Hannan, W. M. Zapar, E. Ahmed, and A. Farghly, "Modeling and analysis of quasi-Z source IMC converter feeding PMSM drive system," *Tikrit Journal of Engineering Sciences*, vol. 32, no. 3, 2025, doi: 10.25130/tjes.32.3.27.

[8] A. Singh *et al.*, "A novel 7-level SCMLI with selective harmonic elimination via war strategy optimization," *Results in Engineering*, vol. 27, p. 105765, Sep. 2025, doi: 10.1016/j.rineng.2025.105765.

[9] H. Sun, B. Wang, W. Li, C. Yang, W. Wei, and B. Zhao, "Research on inertia system of frequency response for power system with high penetration electronics," *Zhongguo Dianji Gongcheng Xuebao/Proceedings of the Chinese Society of Electrical Engineering*, vol. 40, no. 16, pp. 5179–5191, 2020, doi: 10.13334/j.0258-8013.pcsee.200493.

[10] V. Trovato, "The impact of spatial variation of inertial response and flexible inter-area allocation of fast frequency response on power system scheduling," *Electric Power Systems Research*, vol. 198, p. 107354, Sep. 2021, doi: 10.1016/j.epsr.2021.107354.

[11] D. Al Kez, A. M. Foley, and D. J. Morrow, "Analysis of fast frequency response allocations in power systems with high system non-synchronous penetrations," *IEEE Transactions on Industry Applications*, vol. 58, no. 3, pp. 3087–3101, 2022, doi: 10.1109/TIA.2022.3160997.

[12] J. Hui *et al.*, "Frequency coordination control strategy for large-scale wind power transmission systems based on hybrid DC transmission technology with deep Q network assistance," *Applied Sciences (Switzerland)*, vol. 14, no. 15, p. 6817, 2024, doi: 10.3390/app14156817.

[13] Y. Liu, Q. Xie, and H. Liang, "Frequency regulation control strategy for flexible DC transmission system based on adaptive virtual inertia," *Dianli Xitong Zidonghua/Automation of Electric Power Systems*, vol. 45, no. 5, pp. 129–136, 2021, doi: 10.7500/AEPS20200519011.

[14] H. Zhang, W. Xiang, W. Lin, and J. Wen, "Grid forming converters in renewable energy sources dominated power grid: Control strategy, stability, application, and challenges," *Journal of Modern Power Systems and Clean Energy*, vol. 9, no. 6, pp. 1239–1256, 2021, doi: 10.35833/MPCE.2021.000257.

[15] A. Khan, D. A. Aragon, M. Seyedmahmoudian, S. Mekhilef, and A. Stojcevski, "Inertia emulation control of PMSG-based wind turbines for enhanced grid stability in low inertia power systems," *International Journal of Electrical Power and Energy Systems*, vol. 156, 2024, doi: 10.1016/j.ijepes.2023.109740.

[16] J. Mei *et al.*, "A hybrid MMC control strategy to enhance the resilience of DC transmission system," *IEEE Transactions on Industrial Electronics*, vol. 71, no. 9, pp. 10930–10939, 2024, doi: 10.1109/TIE.2023.3344814.

[17] X. Wang, Z. Zhong, W. Jiang, and X. Zhao, "Consensus-based secondary frequency control for parallel virtual synchronous generators," *Sustainable Energy, Grids and Networks*, vol. 38, p. 101341, Jun. 2024, doi: 10.1016/j.segan.2024.101341.

[18] J. Zhu, C. D. Booth, G. P. Adam, A. J. Roscoe, and C. G. Bright, "Inertia emulation control strategy for VSC-HVDC transmission systems," *IEEE Transactions on Power Systems*, vol. 28, no. 2, pp. 1277–1287, 2013, doi: 10.1109/TPWRS.2012.2213101.

[19] J. Zhu *et al.*, "Coordinated flexible damping mechanism with inertia emulation capability for MMC-MTDC transmission systems," *IEEE Journal of Emerging and Selected Topics in Power Electronics*, vol. 9, no. 6, pp. 7329–7342, 2021, doi: 10.1109/JESTPE.2020.3025690.

[20] Q. Liu, Y. Wu, X. Tian, L. Zhu, J. Yan, and C. Chi, "Self-synchronization decoupling control strategy for improving inertia support capability of MMC-HVDC transmission system," in *Proceedings of 2023 IEEE 5th International Conference on Civil Aviation Safety and Information Technology, ICCASIT 2023*, 2023, pp. 1271–1275, doi: 10.1109/ICCASIT58768.2023.10351574.

[21] R. Yang, G. Shi, C. Zhang, G. Li, and X. Cai, "Internal energy based grid-forming control for MMC-HVDC systems with wind farm integration," *IEEE Transactions on Industry Applications*, vol. 59, no. 1, pp. 503–512, Jan. 2023, doi: 10.1109/TIA.2022.3205569.

[22] A. Singh, V. Jately, P. Kala, R. Singhal, and Y. Yang, "Selective harmonic Elimination using Dwarf mongoose optimization in Single-Phase Seven-Level switched capacitor inverter with reduced components," *AEU - International Journal of Electronics and Communications*, vol. 195, 2025, doi: 10.1016/j.aeue.2025.155768.

[23] H. Zhang, W. Xiang, and J. Wen, "Dual grid-forming control with energy regulation capability of MMC-HVDC system integrating offshore wind farms and weak grids," *IEEE Transactions on Power Systems*, vol. 39, no. 1, pp. 261–272, 2024, doi: 10.1109/TPWRS.2023.3244807.

[24] H. Zhang, W. Xiang, Y. He, and J. Wen, "Optimal energy utilization of MMC-HVDC system integrating offshore wind farms for onshore weak grid inertia support," *IEEE Transactions on Power Systems*, vol. 39, no. 1, pp. 1304–1318, 2024, doi: 10.1109/TPWRS.2023.3239166.

[25] S. Yang, J. Fang, Y. Tang, H. Qiu, C. Dong, and P. Wang, "Modular multilevel converter synthetic inertia-based frequency support for medium-voltage microgrids," *IEEE Transactions on Industrial Electronics*, vol. 66, no. 11, pp. 8992–9002, 2019, doi: 10.1109/TIE.2018.2890491.

[26] H. Kim *et al.*, "Exploiting redundant energy of MMC-HVDC to enhance frequency response of low inertia AC Grid," *IEEE Access*, vol. 7, pp. 138485–138494, 2019, doi: 10.1109/ACCESS.2019.2942852.

[27] C. Cardozo *et al.*, "Promises and challenges of grid forming: transmission system operator, manufacturer and academic view points," *Electric Power Systems Research*, vol. 235, p. 110855, 2024, doi: 10.1016/j.epsr.2024.110855.

[28] X. Ma, Y. Lu, J. Tian, and N. Wang, "Key technologies and challenges of grid-forming control for flexible DC transmission system," *Dianli Xitong Zidonghua/Automation of Electric Power Systems*, vol. 47, no. 3, pp. 1–11, 2023, doi: 10.7500/AEPS20220616006.
[29] D. Jovcic, *High Voltage Direct Current Transmission: Converters, Systems and DC Grids*. Wiley, 2019, doi: 10.1002/9781119566632.
[30] H. Zhang, W. Xiang, and J. Wen, "Active energy control of offshore wind power MMC-HVDC system to handle AC faults of receiving-end power grid," *Zhongguo Dianji Gongcheng Xuebao/Proceedings of the Chinese Society of Electrical Engineering*, vol. 43, no. 12, pp. 4600–4613, 2023, doi: 10.13334/j.0258-8013.pcsee.220408.

BIOGRAPHIES OF AUTHORS

Dunya Sh. Wais was born in Baghdad, Iraq, in 1982. She received her B.Sc. degree in electrical engineering (Rank 1) from the College of Engineering Al-Mustansiriyah University, Baghdad, Iraq, in 2005. She received a Master of Science (M.Sc.) in electrical engineering science from Al-Mustansiriyah University, Baghdad, Iraq, in 2021. Her research interests include intelligent optimization, renewable energy, power electronics, power systems, DC-DC converters, AC drive systems, and Arduino applications. She is an assistant lecturer at the Department of Electrical Engineering, College of Engineering, Mustansiriyah University, Baghdad, Iraq. She can be contacted at email: dunya.sh.wais@uomustansiriyah.edu.iq.

Huda A. Abbood was born in Amarah, Iraq, in 1988. She received her B.Sc. degree in electrical engineering (Rank 1) from Electro-Mechanical Engineering Department University of Technology, Baghdad, Iraq in 2011. She received a Master of Science (M.Sc.) in electrical engineering science from Wasit University in 2021. Her research interests include antennas, tunable antennas, IoT, energy harvesting antennas, control modelling, and embedded systems. She is an assistant lecturer at the Department of Electrical Engineering, College of Engineering, Mustansiriyah University, Baghdad, Iraq. She can be contacted at email: hudaabdulameer@uomustansiriyah.edu.iq.